Pb$_2$(SeO$_3$)(SiF$_6$): the first selenite fluorosilicate with a wide bandgap and large birefringence achieved through perfluorinated group modification

Peng-Fei Li,[a,b] Chun-Li Hu,[a,b] Jiang-Gao Mao[a,b] and Fang Kong[*,a,b]

[a] State Key Laboratory of Structural Chemistry, Fujian Institute of Research on the Structure of Matter, Chinese Academy of Sciences, Fuzhou 350002, P. R. China.

[b] University of Chinese Academy of Sciences, Beijing 100049, P. R. China.

E-mail: kongfang@fjirsm.ac.cn

Supporting Information

S1. Experimental Section

Reagents and Instruments

SeO$_2$ (Adamas-beta, 99.99%), H$_2$SiF$_6$ (Adamas-beta, 30% in water) and Pb(BF$_4$)$_2$ (Adamas-beta, 50% in water) were obtained from commercial sources and used without further purification.

Powder X-ray diffraction (PXRD) patterns of Pb$_2$(SeO$_3$)(SiF$_6$) was collected on the Miniflex 600 powder X-ray diffractometer using Cu Kα radiation (λ = 1.54186 Å) at room temperature in the angular range of 2θ = 10-70° with a scan step size of 0.02°.

The elemental distribution maps and microprobe elemental analyses were carried out with the aid of a field-emission scanning electron microscope (FESEM, JSM6700F) equipped with an energy-dispersive X-ray spectroscope (EDS, Oxford INCA).

IR spectra was carried out on a Magna 750 FT-IR spectrometer using air as background in the range of 4000–400 cm^{-1} with a resolution of 2 cm^{-1} at room temperature.

The UV-vis-NIR spectra was obtained at 2000–200 nm by a PerkinElmer Lambda 900 spectrophotometer using BaSO$_4$ as the reference, and the reflection spectra was converted into an absorption spectrum using the Kubelka-Munk function. Absorption data was calculated from the diffuse reflection data by the Kubelka-Munk function: α/S = (1-R)^2/2R, where α and S represent the absorption coefficient and the scattering coefficient, respectively. The band gap value can be given by extrapolating the

absorption edge to the baseline in the α/S vs. energy graph[1].

Thermogravimetric analyses (TGA) and differential thermal analysis (DTA) were measured by Netzsch STA 499C installation. The samples about 5.0-10.0 mg were placed in alumina crucibles and heated in 20-1200 °C at a rate of 15 K/min under N_2 atmosphere.

The LIDT measurements of the $Pb_2(SeO_3)(SiF_6)$ crystal samples and $AgGaS_2$ samples were performed by a Q-switched pulsed laser. The particle size range of the tested sample was 150−210 μm, the laser wavelength was 1064 nm, the pulse duration was 10 ns, the pulse frequency was 1 Hz, and the laser spot area focused on the sample was 1.54 mm^2. The energy of the laser emission was gradually increased during the measurement, and the LIDT of the sample was determined when it turned black under the laser.

Syntheses

Single crystals of $Pb_2(SeO_3)(SiF_6)$ were successfully obtained by low-hydrothermal reaction. A mixture of SeO_2 (222.2 mg, 2 mmol), H_2SiF_6 (0.25 ml) and $Pb(BF_4)_2$ (3 ml) was sealed in an autoclave containing Teflon liner equipped (23 ml), heated at 105 °C for 7200 minutes, and then slowly cooled to room temperature in 1500 minutes. The products were separated by vacuum filtration, washed with alcohol and dried in air at room temperature. The transparent needle $Pb_2(SeO_3)(SiF_6)$ crystal was obtained in a single pure phase, with a yield of about 29% (based on Se). The elemental distribution map indicates a uniform dispersion of all elements (Figure 1) and its purity has been verified through X-ray diffraction (XRD) studies (Figure S1).

Single-crystal X-ray diffraction

Single crystal X-ray diffraction data of $Pb_2(SeO_3)(SiF_6)$ was obtained on Agilent Technologies SuperNova dual-wavelength CCD diffractometer with a graphite-monochromated Mo Kα radiation (λ = 0.71073 Å) at room temperature. Data reduction and cell refinement and were performed with *CrysAlisPro*. The structure was solved by the direct methods and refined by full-matrix least-squares fitting on F^2 using *Olex2-1.5* crystallographic software package[2, 3]. All of the atoms were refined with anisotropic thermal parameters and finally converged for $F_0^2 \geq 2\sigma(F_0^2)$. The structural data was also checked for possible missing symmetry with the program *PLATON*, and no higher symmetry was found[4, 5]. The detailed crystallographic data for $Pb_2(SeO_3)(SiF_6)$ was given in Table S1. The bond lengths were listed in Table S2.

S2. Computational Method

Single-crystal structural data of $Pb_2(SeO_3)(SiF_6)$ was used for the theoretical calculations. The electronic structures were performed using a plane-wave basis set and pseudo-potentials within density functional theory (DFT) implemented in the total-energy code CASTEP[6]. For the exchange and correlation functional, we chose Perdew–Burke–Ernzerhof (PBE) in the generalized gradient approximation (GGA)[7]. The interactions between the ionic cores and the electrons were described by the ultrasoft pseudopotential[8]. The following valence-electron configurations were considered in the computation: $Se-4s^2 4p^4$, $Si-3s^2 3p^2$, $Pb-5d^{10} 6s^2 6p^2$, $F-2s^2 2p^5$ and $O-2s^2 2p^4$. The numbers of plane waves included in the basis sets were determined by cutoff energy of 850 eV for $Pb_2(SeO_3)(SiF_6)$. The numerical integration of the Brillouin zone was performed using Monkhorst-Pack k-point sampling of $2 \times 5 \times 3$ for $Pb_2(SeO_3)(SiF_6)$. The other parameters and convergent criteria were the default values of CASTEP code.

Calculated method of linear optical response properties

The calculations of linear optical properties in terms of the complex dielectric function $\varepsilon(\omega) = \varepsilon_1(\omega) + i\varepsilon_2(\omega)$ were made. The imaginary part of the dielectric function ε_2 was given in the following equation:

$$\varepsilon^{ij}_2(\omega) = \frac{8\pi^2 h^2 e^2}{(m^2 V)} \sum_k \sum_{cv} (f_c - f_v) \frac{p^i_{cv}(k) p^j_{cv}(k)}{E^2_{vc}} \delta[E_c(k) - E_v(k) - h\omega]$$

The f_c and f_v represent the fermi distribution functions of the conduction and valence band. The term $p^i_{cv}(k)$ denotes the momentum matrix element transition from the energy level c of the conduction band to the level v of the valence band at the kth

point in the Brillouin zone (BZ), and V is the volume of the unit cell.

The real part $\varepsilon_1(\omega)$ of the dielectric function $\varepsilon(\omega)$ follows from the Kramer–Kronig relationship. All the other optical constants may be derived from $\varepsilon_1(\omega)$ and $\varepsilon_2(\omega)$. For example, the refractive index n(ω) can be calculated using the following expression[7]:

$$n(\omega)=(\frac{1}{\sqrt{2}})[\sqrt{\varepsilon_1^2(\omega) + \varepsilon_2^2(\omega)} + \varepsilon_1(\omega)]^{1/2}$$

Table S1. Summary of crystal data and structural refinements for $Pb_2(SeO_3)(SiF_6)$.

molecular formula	$Pb_2(SeO_3)(SiF_6)$
Formula Weight	683.43
crystal system	orthorhombic
space group	*Pnma*
Temperature(K)	100.15
F(000)	1160.0
a/Å	13.8153(4)
b/Å	5.4470(2)
c/Å	9.6098(3)
α(deg)	90
β(deg)	90
γ(deg)	90
V/Å^3	723.16(4)
Z	4
Dc(g.cm^{-3})	6.277
GOF on F^2	1.030
R_1, $wR_2[I > 2\sigma(I)]^a$	$R_1 = 0.0189$, $wR_2 = 0.0459$
R_1, wR_2 (all data)^a	$R_1 = 0.0199$, $wR_2 = 0.0465$

$^aR_1 = \sum||F_o| - |F_c||/\sum|F_o|$, $wR_2 = \{\sum w[(F_o)^2 - (F_c)^2]^2/\sum w[(F_o)^2]^2\}^{1/2}$

Table S2. Calculated bond valences for $Pb_2(SeO_3)(SiF_6)$.

| Compound	Bond	Bond lengths	Bond-valence	BVS
$Pb_2(SeO_3)(SiF_6)$	Se(1)-O(1)	1.727(4)	1.255	3.958
	Se(1)-O(1)#1	1.727(4)	1.255	
	Se(1)-O(2)	1.674(7)	1.448	
	Si(1)-F(1)	1.679(4)	0.765	4.513
	Si(1)-F(1)#2	1.679(4)	0.765	
	Si(1)-F(2)	1.699(6)	0.725	
	Si(1)-F(3)	1.674(6)	0.776	
	Si(1)-F(4)	1.691(4)	0.741	
	Si(1)-F(4)#2	1.691(4)	0.741	
	Pb(1)-O(1)	2.505(4)	0.346	1.374
	Pb(1)-O(1)#3	2.515(4)	0.346	**1.868**
	Pb(1)-O(1)#4	2.515(4)	0.336	
	Pb(1)-O(1)#1	2.505(4)	0.346	
	Pb(1)-F(2)	**2.809**	**0.122**	
	Pb(1)-F(2)	**2.809**	**0.122**	
	Pb(1)-F(3)	**2.964**	**0.080**	
	Pb(1)-F(4)	**2.941**	**0.085**	
	Pb(1)-F(4)	**2.941**	**0.085**	
	Pb(2)-O(1)#5	2.689(4)	0.210	1.443
	Pb(2)-O(1)#6	2.689(4)	0.210	**1.755**
	Pb(2)-O(2)	2.595(7)	0.271	
	Pb(2)-F(1)	2.589(4)	0.221	
	Pb(2)-F(1)#1	2.589(4)	0.221	
	Pb(2)-F(4)#7	2.719(4)	0.155	
	Pb(2)-F(4)#8	2.719(4)	0.155	
	Pb(2)-F(3)	**2.911**	**0.092**	
	Pb(2)-O(2)	**2.928**	**0.110**	
	Pb(2)-O(2)	**2.928**	**0.110**	

Bold font: Longer Pb-O and Pb-F bonds are considered.

Symmetry transformations used to generate equivalent atoms:

#1 +X,1/2-Y,+Z; #2 +X,3/2-Y,+Z; #3 1-X,1-Y,-Z; #4 1-X,-1/2+Y,-Z; #5 1-X,1-Y,1-Z; #6 1-X,-1/2+Y,1-Z; #7 3/2-X,-1/2+Y,1/2+Z; #8 3/2-X,1-Y,1/2+Z;

Table S3. State energies (eV) of the lowest conduction band (L-CB) and the highest valence band (H-VB) of $Pb_2(SeO_3)(SiF_6)$.

k-point	L-CB	H-VB
G (0.000, 0.000, 0.000)	4.169569	0
Z (0.000, 0.000, 0.500)	4.560663	-0.087824
T (-0.500, 0.000, 0.500)	4.612347	-0.090364
Y (-0.500, 0.000, 0.000)	4.210380	-0.004641
S (-0.500, 0.500, 0.000)	4.589767	-0.171739
X (0.000, 0.500, 0.000)	4.531338	-0.141615
U (0.000, 0.500, 0.500)	4.301404	-0.149858
R (-0.500, 0.500, 0.500)	4.328070	-0.171864
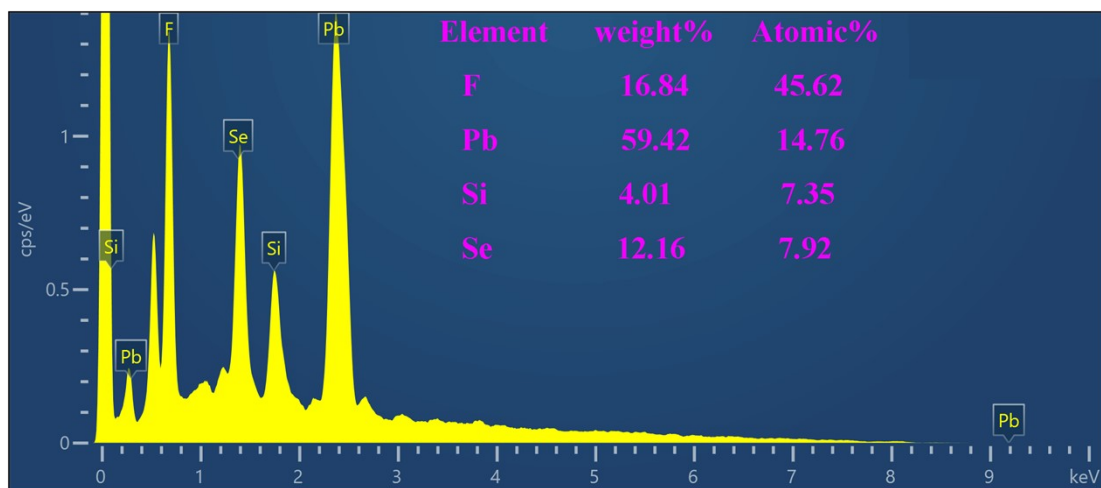
(a)
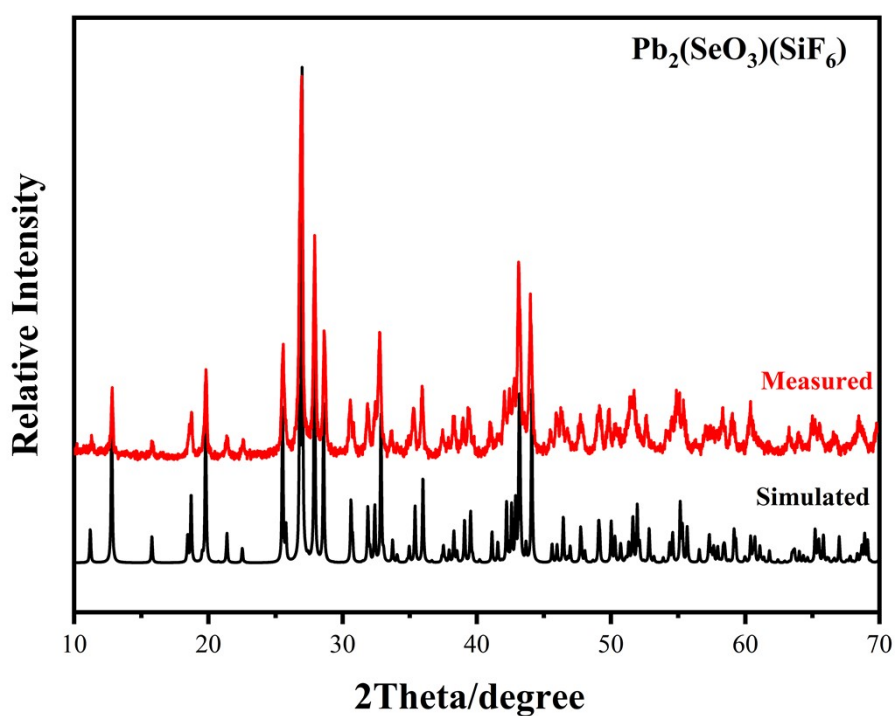
(b)

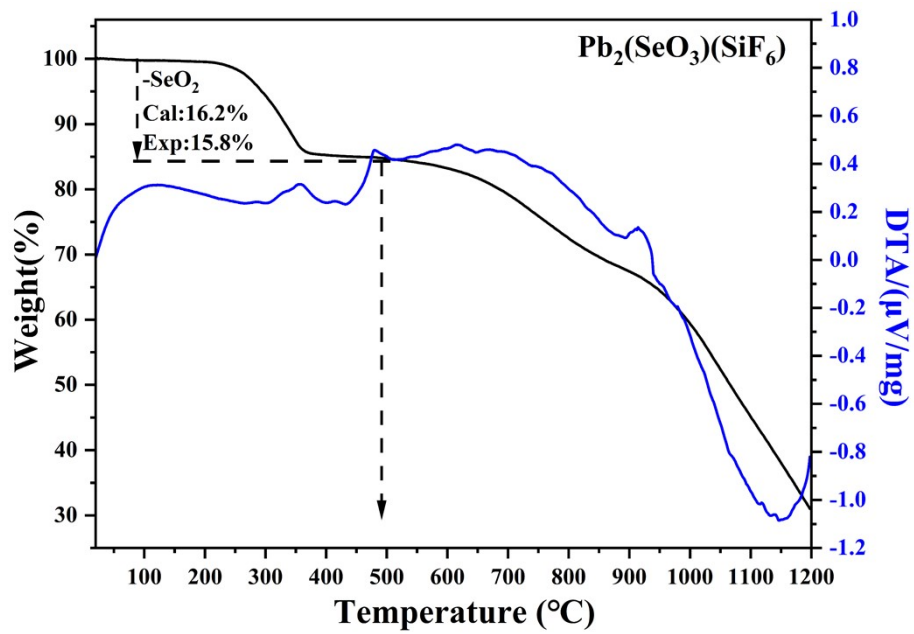**Figure S1.** The quantitative element analysis results (a) and the XRD powder patterns (b) of $Pb_2(SeO_3)(SiF_6)$.

Figure S2. TGA and DTA results of $Pb_2(SeO_3)(SiF_6)$.
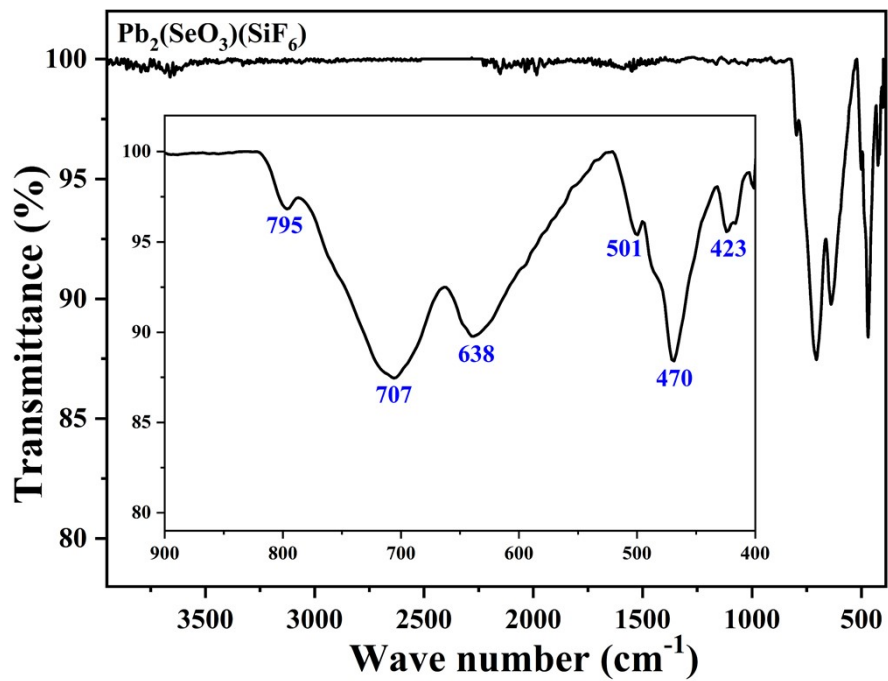
Figure S3. IR spectrum of $Pb_2(SeO_3)(SiF_6)$.

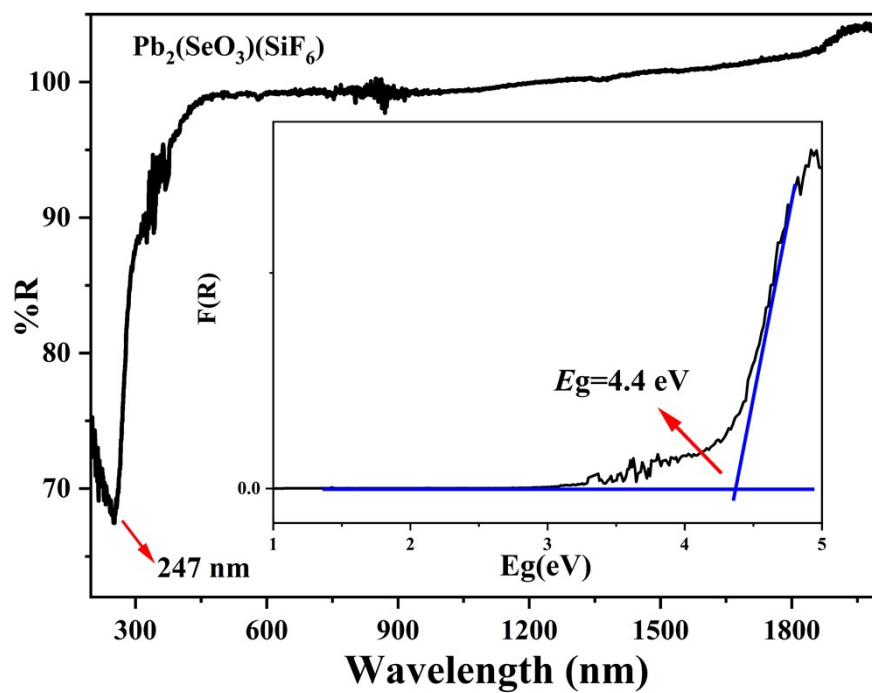**Figure S4.** UV−vis−NIR diffuse-reflectance spectrum of $Pb_2(SeO_3)(SiF_6)$.

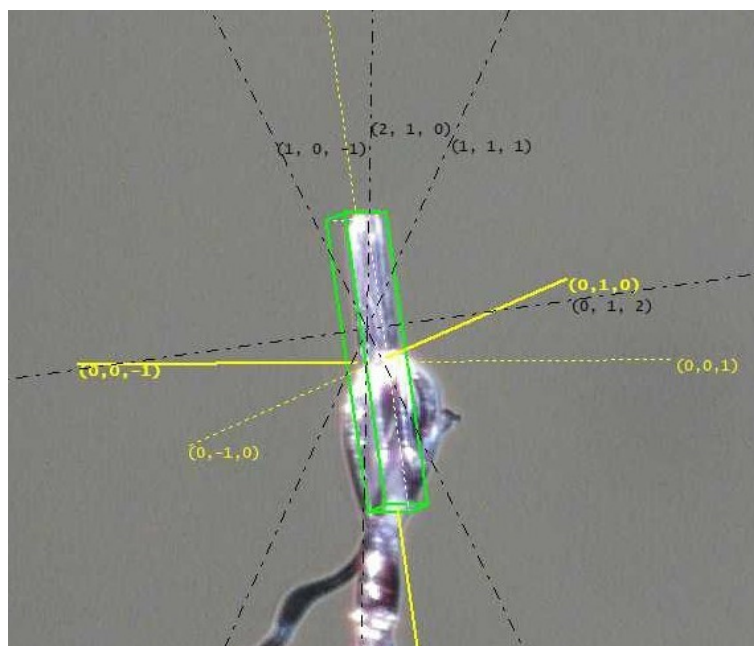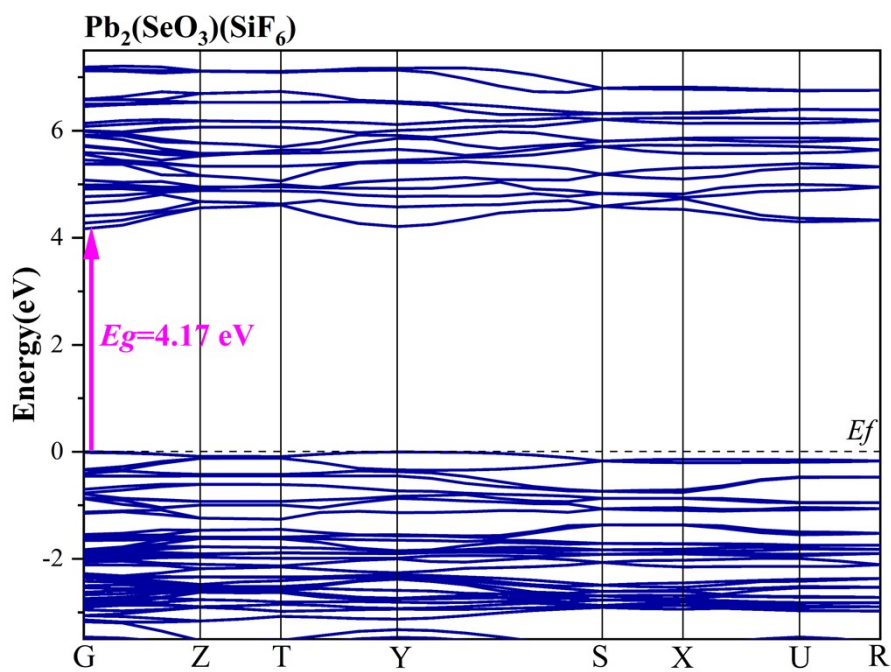**Figure S5.** Crystal plane indexing of $Pb_2(SeO_3)(SiF_6)$.

Figure S6. Band structure of $Pb_2(SeO_3)(SiF_6)$.

References

[1] P. Kubelka, F. Munk, An Article on Optics of Paint Layers, Technol. Physical 12 (1931) 259−274.

[2] G.M. Sheldrick, Crystal structure refinement with SHELXL, Acta Cryst., C71 (2015) 3-8.

[3] O.V. Dolomanov, L.J. Bourhis, R.J. Gildea, J.A.K. Howard, H. Puschmann, OLEX2: a complete structure solution, refinement and analysis program, J. Appl. Cryst., 42 (2009) 339-341.

[4] R.H. Blessing, An empirical correction for absorption anisotropy, Acta Cryst., A51 (1995) 33−38.

[5] A.L. Spek, Single-crystal structure validation with the program PLATON, J. Appl. Cryst., 36 (2003) 7−13.

[6] M.D. Segall, P.J.D. Lindan, M.J. Probert, C.J. Pickard, P.J. Hasnip, S.J. Clark, M.C. Payne, First-principles simulation: ideas, illustrations and the CASTEP code, Phys-Condens Mat., 14 (2002) 2717-2744.

[7] V. Milman, B. Winkler, J.A. White, C.J. Pickard, M.C. Payne, E.V. Akhmatskaya, R.H. Nobes, Electronic structure, properties, and phase stability of inorganic crystals: A pseudopotential plane-wave study, Int. J. Quantum. Chem., 77 (2000) 895-910.

[8] J.P. Perdew, K. Burke, M. Ernzerhof, Generalized Gradient Approximation Made Simple, Phys. Rev. Lett., 77 (1996) 3865-3868.